minerals

MDPI

Article

Multiple-Stage Neoproterozoic Magmatism Recorded in the Zhangbaling Uplift of the Northeastern Yangtze Block: Evidence from Zircon Ages and Geochemistry

Jing Wang [1,2], Jun He [1,*], Jingxin Zhao [1], Yizeng Yang [3] and Fukun Chen [1]

[1] School of Earth and Space Sciences, University of Science and Technology of China, Hefei 230026, China
[2] Geological Survey of Anhui Province, Hefei 230001, China
[3] School of Environment and Tourism, West Anhui University, Lu'an 237012, China
* Correspondence: jhe1989@ustc.edu.cn

Abstract: The Yangtze Block records Neoproterozoic magmatism and sedimentation related to the breakup of Rodinia and is an important piece in the reconstruction of the supercontinent. However, the tectonic setting and position of this block in Rodinia remain a subject of debate. In the present study, we report the zircon U-Pb ages and Hf isotopic composition of zircon and geochemical and Nd-Pb isotopic compositions for meta-volcanic rocks exposed in the Zhangbaling uplift of the NE Yangtze Block. The volcanic rocks, dominated by rhyolite and dacite, belong to the calc-alkaline series and show geochemical characteristics of arc rocks. Zircon U-Pb isotopic ages show that volcanic rocks in the Xileng Formation formed at ca. 790 Ma and ca. 760–700 Ma peaking at ~740 Ma. The late-stage volcanism was widely exposed in the uplift, characterized by a temporal-spatial trend becoming younger southwards. The old volcanic rocks have low initial ε_{Nd} (−11.0) and ε_{Hf} (−19.7 to −8.2) values and low Pb isotopic ratios, likely indicating an origin from ancient basement rocks underneath the Yangtze Block. The younger ones, being similar to continental arc andesite in trace element compositions, have relatively high initial ε_{Nd} (mostly −4.6 to 0.5) and ε_{Hf} (−0.4 to 8.8) values and high Pb isotopic ratios. These isotopic features point to an origin from the partial melting of juvenile crustal rocks. Sedimentary rocks of the Xileng Formation and the overlying strata also contain numerous zircon grains of ~700 Ma to ~630 Ma. The volcanic rocks in the Zhangbaling uplift might demonstrate long-lasting subduction along the northeastern margin of the Yangtze Block, probably active until ca. 700 Ma.

Keywords: Rodinia; volcanism; geochemistry; zircon age; Nd-Hf-Pb isotopes

Citation: Wang, J.; He, J.; Zhao, J.; Yang, Y.; Chen, F. Multiple-Stage Neoproterozoic Magmatism Recorded in the Zhangbaling Uplift of the Northeastern Yangtze Block: Evidence from Zircon Ages and Geochemistry. *Minerals* **2023**, *13*, 562. https://doi.org/10.3390/min13040562

Academic Editors: William L. Griffin and Ilya Bindeman

Received: 28 February 2023
Revised: 31 March 2023
Accepted: 15 April 2023
Published: 17 April 2023

1. Introduction

The Yangtze Block, a part of South China, preserves well Neoproterozoic magmatism and sedimentation related to the breakup of Rodinia and, hence, is important for the supercontinent reconstruction. Over the past decades, the genesis and tectonic evolution of the extensive Neoproterozoic igneous rocks within this block have received considerable attention. However, there are still debates, especially on the coeval tectonic setting, including three competing models of plume-rift, slab-arc, and plate-rift [1–5]. The position of the South China Block in Rodinia reconstruction also remains unclear [2,6–9]. Scholars have proposed that the South China Block was originally placed in the interior of Rodinia [1,2,6] or adjacent to India and East Antarctica during the breakup of Rodinia to the Gondwana assembly in the Neoproterozoic [9–11].

Low-grade metamorphosed sedimentary and volcanic rocks of Neoproterozoic ages are widely exposed in the Zhangbaling uplift of the northeastern Yangtze Block. They are termed the Zhangbaling Group and distributed along the Tan-Lu fault zone within Anhui Province. These rocks were correlated with low-T/high-P metamorphic rocks in the Dabie-Sulu orogenic belt, such as the Hongan Group and the Yuntai Formation of the Haizhou

Group [12,13]. The Zhangbaling Group is also an important object for understanding the tectonic evolution of the Yangtze Block during the Neoproterozoic. The age of Zhangbaling volcano-sedimentary rocks was previously interpreted as Paleo- to Mesoproterozoic [14], early Neoproterozoic (975–925 Ma) [15,16], or middle Neoproterozoic (770–720 Ma) [17–19]. Therefore, the ages of these meta-volcanic and meta-sedimentary rocks still need to be precisely constrained for clarifying the tectonic evolution of the Yangtze Block. In the present study, we report the U-Pb ages and Hf isotopic composition of zircon and bulk rock geochemical and Nd-Pb isotopic compositions of meta-volcanic rocks from the Zhangbaling uplift in the northeastern Yangtze Block, and discuss the nature of the magmas, magmatic and crustal evolution, and their tectonic relationship with Rodinia.

2. Geological Setting and Samples

The Yangtze Block is one of the most important tectonic units in China. This block collided with the North China Block along the Qinling-Dabie-Sulu orogenic belt in the Early Mesozoic [20]. The Dabie and Sulu orogenic belts were later offset by the Tan-Lu fault zone for ca. 350 km [21,22]. The Zhangbaling uplift, named after the wide exposure of greenschist-facies metamorphosed volcano-sedimentary rocks of the Zhangbaling Group, is located between the Dabie and Sulu belts along the Tan-Lu fault zone in eastern China and strikes NNE-ward with a length of ca. 150 km (Figure 1).

The Zhangbaling Group is exposed mainly in the northern segment of the uplift, locally on the eastern side of the southern Zhangbaling uplift, and sporadically along the southeastern edge of the Dabie orogenic belt (Figure 1). The major outcrops are located mainly in the Chuzhou, Chaohu, Lujiang, and Susong areas from north to south. The Zhangbaling Group was subdivided into the Beijiangjun and Xileng formations bottom to top (Figure 2). The Xileng Formation unconformably overlies the Beijiangjun Formation and previously was considered to be the upper part of this group. The Beijiangjun Formation consists mainly of low greenschist-facies metamorphosed clastic rocks, with major rock types of phyllite and meta-sandstone. The Xileng Formation is dominated by medium to high greenschist-facies metamorphosed intermediate volcanic rocks with major rock types of keratophyre, quartz keratophyre, and quartz schist. From bottom to top, it can be further subdivided into a white mica schist unit, a quartz-feldspar schist unit, and a blue amphibole schist unit [23]. The Xileng Formation is unconformably overlain by the Zhougang Formation, which is composed of low greenschist-facies rocks dominated by phyllite, pebble-bearing phyllite, and meta-sandstone.

We have systematically investigated low-grade metamorphosed volcanic rocks of the Xileng Formation. Seventeen samples were collected from different areas of the Zhangbaling uplift, including the Chuzhou, Chaohu, Lujiang, and Susong areas. These samples are mainly quartz keratophyre with minor keratophyre and quartz schist. The quartz keratophyres are mainly light gray in color with porphyritic textures and massive structures. They consist mainly of quartz (~40 vol.%–50 vol.%) and albite (~40 vol.%–50 vol.%) and their matrix is composed of microcrystalline albite (~40 vol.%–50 vol.%), quartz (~30 vol.%–40 vol.%), and sericite (~5 vol.%–10 vol.%). The quartz schists are mainly grayish-white in color with crystalloblastic texture and medium-bedded structure. They are composed mainly of quartz (~50 vol.%–60 vol.%), albite (~30 vol.%–35 vol.%), and sericite (~10 vol.%).

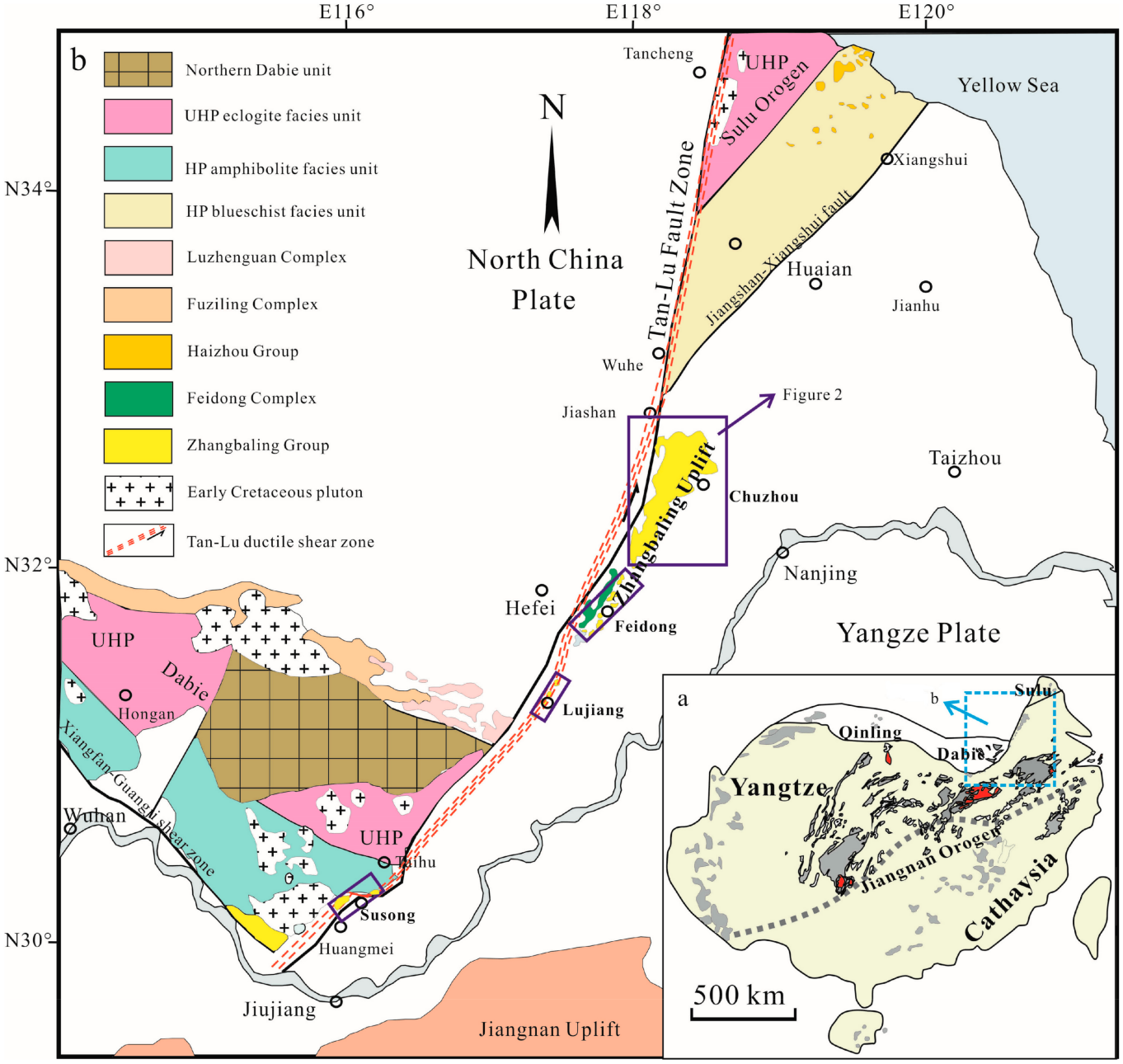

Figure 1. (**a**) Sketch map of the Sorth China Plate; (**b**) Simplified geological map in the southern Tan-Lu fault zone after [17]. HP: high pressure; UHP: ultra-high pressure.

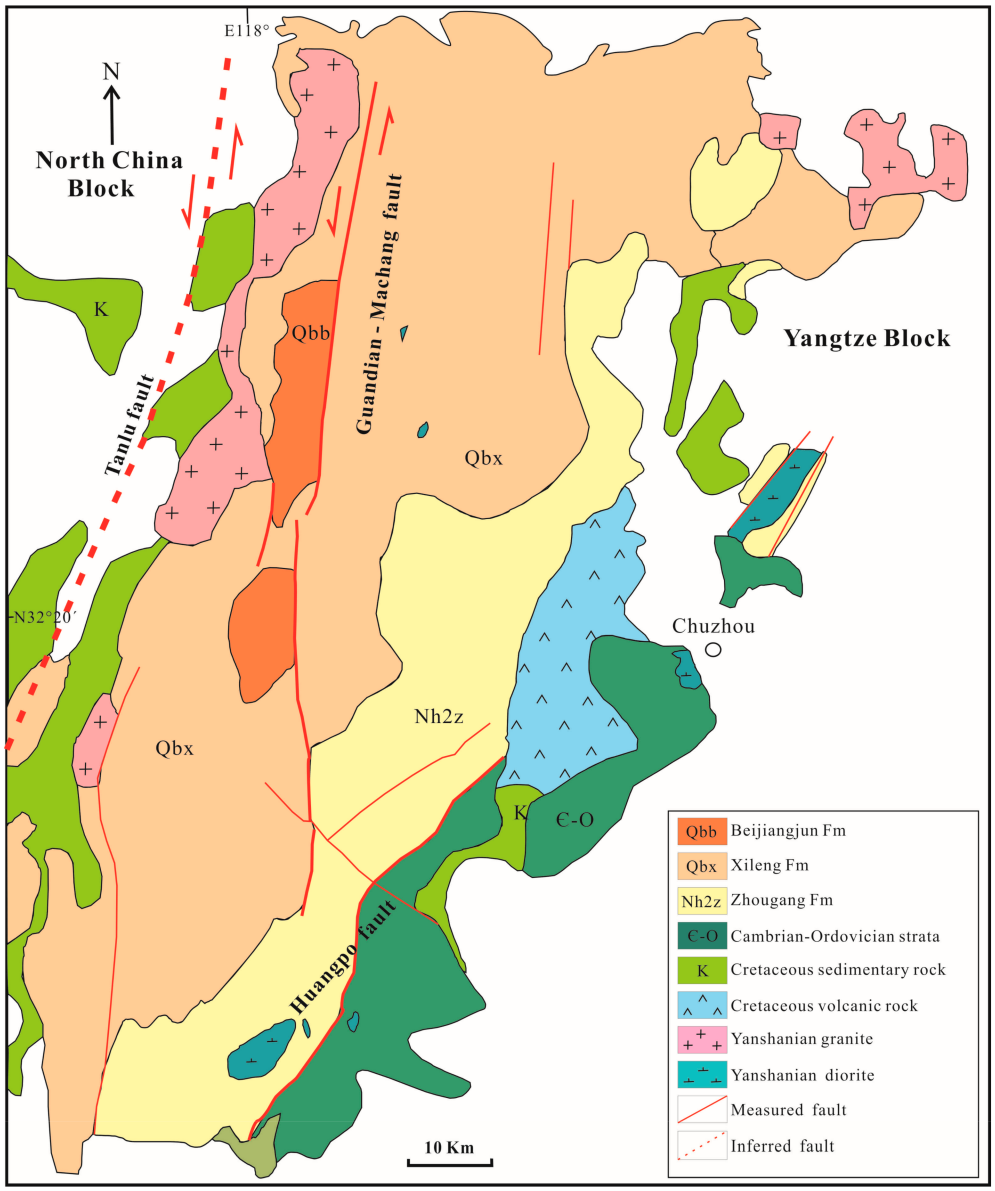

Figure 2. Simplified geological map of the northern Zhangbaling uplift after [24].

3. Analytical Methods

Rock samples of about 5 kg in weight were crushed for the zircon separation and fresh crushed pieces of ~20 g were milled for whole-rock powder in an alloy mortar. The contents of major elements were analyzed in fused lithium borate glass beads by X-ray florescence spectrometry (XRF) at the Guangzhou Institute of Geochemistry, Chinese Academy of Sciences CAS. Calibration lines used in the quantification were produced by a bivariate regression of data from 36 reference materials encompassing a wide range of silicate compositions, and analytical uncertainties were between 1% and 5%. The contents of trace elements were analyzed on an Agilent 7500a ICP-MS in the Key Laboratory of Crust-Mantle Materials and Environments, University of Science and Technology of China (USTC). Powdered samples were dried at 105 °C for 4 h. To achieve complete dissolution, ~50 mg of material was dissolved in a mixture of HF + HNO_3 solution in Teflon bombs at 190 °C for 72 h. Dissolved samples were then diluted to 80 mL by the addition of 2% HNO_3 solution prior to the analysis. The precision and accuracy of the analyses were better than 5% for trace elements, as estimated by analysis of the USGS rock standards BHVO−2 and AGV-2. Analyses of whole-rock Sm-Nd and Pb isotopic composition were performed at the

Laboratory for Radiogenic Isotope Geochemistry, USTC. Elements were isolated from each other by standard chromatographic separation techniques. Measured Nd isotopic ratios were normalized to $^{146}Nd/^{144}Nd$ of 0.7219. Standard solutions of NBS987 for Sr and La Jolla for Nd were measured during the analysis. The precision of the $^{147}Sm/^{144}Nd$ ratios was better than 0.5%. The precision of the measured Pb isotopic ratios was better than 0.01%. Further details on the analytical procedures are described elsewhere [25].

Zircon grains were extracted from rock samples by standard crushing, sieving, heavy liquids, and magnetic separation techniques. Transparent zircon grains without cracks were subsequently handpicked under a binocular microscope, mounted in epoxy resin, and then polished down to expose grain centers. Prior to the U-Pb isotopic dating, zircon crystals were imaged by the cathodoluminescence (CL) technique. CL image and zircon U-Pb dating were performed at the USTC. The detailed analytical procedures are reported elsewhere [26]. Zircon 91500 was used as an external standard to correct isotopic fractionation during analysis. NIST610 was used as an external standard to normalize the U, Th, and Pb contents of the unknowns. Raw data were processed using the GLITTER program [27]. A common Pb correction was applied using the Andersen method [28]; data were then calculated and plotted using the ISOPLOT program [29]. The uncertainties of individual analyses were reported at the 1σ level and weighted average ages were calculated at the 2σ level. Zircon Hf isotopic analysis was performed using a double-focusing multi-collector Neptune MC-ICP mass spectrometer at USTC. Analytical procedures are given elsewhere [30]. A $^{175}Lu/^{176}Lu$ value of 0.02655 was used for the isotopic fractionation correction. Isobaric interference of ^{176}Yb on ^{176}Hf was corrected using the mean fractionation index of Iizuka [31]. A $^{176}Hf/^{177}Hf$ value of 0.282007 ± 7 (2σ, n = 36) was obtained for the standard zircon GJ1.

4. Results

4.1. Zircon U-Pb Isotopic Ages and Hf Isotopic Composition

Eight volcanic rock samples of the Zhangbaling Group, collected from different localities, were selected for the zircon U-Pb isotopic dating, including three from Chuzhou and two from Feidong in the north, one from Lujiang and two from Susong in the south. The analytical results are given in the Table S1 in Supplementary Materials and are summarized in Table 1. Most zircon grains from meta-volcanic rocks are colorless and transparent, and euhedral to subhedral, with sizes ranging from 100 μm to 200 μm in length, with length-to-width ratios between 1:1 and 3:1. In the CL images, most of the grains exhibit weak to clear oscillatory zoning (Figure S1 in Supplementary Materials). In general, the analyzed grains had variable U (14–410 ppm) and Th contents (6–3580 ppm), but all of them had high Th/U ratios of 0.33–6.11, indicating magmatic origin [32,33]. In this study, $^{206}Pb/^{238}U$ ages are used for zircon grains younger than 1.0 Ga and $^{207}Pb/^{206}Pb$ ages for the older ones [34].

Table 1. Summary of zircon ages and Nd-Hf isotopic compositions for volcanic rocks of the Xileng Formation in the Zhangbaling uplift.

Sample No.	Sampling Area	Total Number of Grains	Major Age Group (Ma)	Zircon $\varepsilon_{Hf}(t)$ Value	Whole-Rock $\varepsilon_{Nd}(t)$ Value
Early-stage					
XL02	Chuzhou	60	~3300–2000, 790 ± 11	−19.7 to −8.2	−11.03
Late-stage					
XL06	Chuzhou	32	791 ± 10, 741 ± 7	−0.4 to +8.8	−3.34
XL13	Chuzhou	32	795 ± 7, 746 ± 6		−2.54
XL15	Feidong	33	789 ± 11, 732 ± 6		−1.73
XL17	Feidong	28	790 ± 11, 747 ± 16		−0.19
XL18	Lujiang	32	789 ± 8, 738 ± 7		−1.86
XL23	Susong	32	791 ± 15, 736 ± 7	+1.3 to +6.1	+0.49
XL24	Susong	32	797 ± 9, 739 ± 8		−4.13

Chuzhou area: Sixty grains from sample XL02 were analyzed, but some of them were discarded for being highly discordant (Figure 3a). Fifty-two grains gave U-Pb isotopic ages ranging from 3390 ± 29 Ma to 129 ± 3 Ma. Broadly, these concordant analyses fell into three age populations according to their $^{206}Pb/^{238}U$ or $^{207}Pb/^{206}Pb$ ages. Thirty grains yielded Paleo-Archean to Paleo-Proterozoic ages of 3390 ± 29 Ma to 2026 ± 61 Ma, with a minor peak at ~2.5 Ga. They can be interpreted as captured zircon grains, indicating the existence of ancient basement rocks underneath the Yangtze Block. Seventeen grains gave Neoproterozoic ages of 922 ± 15 Ma to 670 ± 13 Ma, and fifteen of them yielded a weighted mean $^{206}Pb/^{238}U$ age of 790 ± 11 Ma (MSWD = 2.5), interpreted as the formation time of this volcanic rock. Five grains had very young ages from 211 ± 6 Ma to 129 ± 3 Ma, perhaps resulting from Pb-loss in late thermal event(s). Twenty-six out of thirty-two grains from sample XL06 had concordant $^{206}Pb/^{238}U$ ages ranging from ~830 Ma to 720 Ma (Figure 3b). Sixteen of them yielded a weighted mean $^{206}Pb/^{238}U$ age of 791 ± 10 Ma (MSWD = 2.9), likely indicating captured grains of an early magmatic event. The remaining ten grains gave younger ages between 757 ± 17 Ma and 723 ± 12 Ma, yielding a weighted mean age of 741 ± 7 Ma (MSWD = 0.7), interpreted as the formation time of quartz keratophyre. Twenty-three out of thirty-two grains from sample XL13 displayed concordant $^{206}Pb/^{238}U$ ages of ~820 Ma to 720 Ma (Figure 3c). They clustered around two age peaks with weighted mean ages of 795 ± 7 Ma (n = 13, MSWD = 1.1) and 746 ±6 Ma (n = 10, MSWD = 0.7). The latter is interpreted as the intrusion age and the former as an early magmatic event recorded in the captured zircon grains.

Feidong area: Twenty-four out of thirty-three grains from sample XL15 had concordant $^{206}Pb/^{238}U$ ages ranging from 830 ± 10 Ma to 688 ± 9 Ma (Figure 3d) and ten of them yielded a weighted mean $^{206}Pb/^{238}U$ age of 789 ± 11 Ma (MSWD = 0.16), indicating an early magmatic event. The remaining fourteen grains gave younger ages between 763 ±11 Ma and 718 ± 7 Ma, yielding a weighted mean age of 732 ± 6 Ma (MSWD = 1.4), interpreted as the formation time of this quartz keratophyre. Sixteen out of twenty-eight grains from sample XL17 had concordant $^{206}Pb/^{238}U$ ages of 815 ± 14 Ma to 254 ± 4 Ma (Figure 3e). They clustered around two age peaks with weighted mean ages of 790 ± 11 Ma (n = 9, MSWD = 1.1) and 747 ± 16 Ma (n = 5, MSWD = 0.5), interpreted as the ages of an early magmatic event and the extrusion of this volcanic rock. Two grains showed extremely young ages of 255 ± 4 Ma and 254 ± 5 Ma, likely representing Pb-loss during a later thermal event.

Lujiang area: Twenty-five out of thirty-two grains from sample XL18 had concordant $^{206}Pb/^{238}U$ ages ranging from 827 ± 19 Ma to 707 ± 10 Ma (Figure 3f). Fifteen grains gave a weighted mean age of 789 ± 8 Ma (MSWD = 1.3), indicating an early magmatic event. The remaining ten grains had younger ages of 754 ± 13 Ma to 721 ± 15 Ma, yielding a weighted mean age of 738 ± 7 Ma (MSWD = 0.7), interpreted as the crystallization time of quartz keratophyre.

Susong area: Twenty-two out of thirty-two grains from sample XL23 had concordant $^{206}Pb/^{238}U$ ages ranging from 814 ± 11 Ma to 683 ± 15 Ma (Figure 3g). Eight grains yielded an old weighted mean $^{206}Pb/^{238}U$ age of 791 ± 15 Ma (MSWD = 1.7), while the other fourteen grains had ages of 748 ± 13 Ma to 720 ± 13 Ma, yielding a weighted mean age of 736 ± 7 Ma (MSWD = 0.3), interpreted as the formation time of this rock. Twenty-three out of thirty-two grains from sample XL24 displayed concordant $^{206}Pb/^{238}U$ ages of 847 ±18 Ma to 697 ± 10 Ma (Figure 3h). They clustered around two age peaks with weighted mean ages of 797 ± 9 Ma (n = 13, MSWD = 1.2) and 739 ± 8 Ma (n = 10, MSWD = 0.7), interpreted as the ages of an early magmatic event and the extrusion of this volcanic rock.

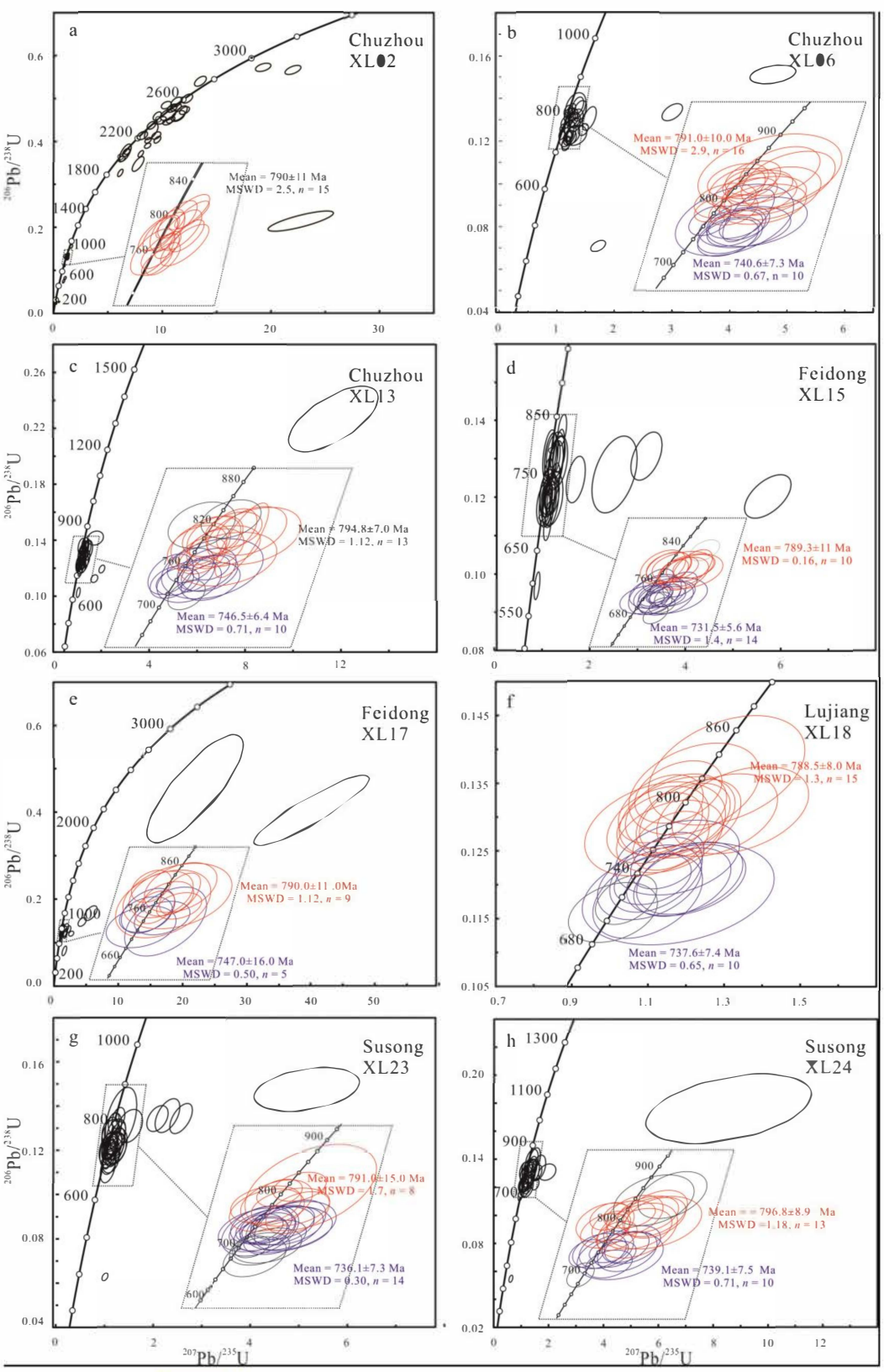

Figure 3. Zircon U-Pb isotopic concordia diagrams for volcanic rocks of the Xileng Formation. (**a**) Early-stage volcanic rocks in Chuzhou; (**b**,**c**) Late-stage volcanic rocks in Chuzhou; (**d**,**e**) Late-stage volcanic rocks in Feidong; (**f**) Late-stage volcanic rocks in Lujiang; (**g**,**h**) Late-stage volcanic rocks in Susong.

Zircon grains from three meta-volcanic rock samples of the Xileng Formation were analyzed for Hf isotopic composition. The analytical results are given in the Table S2 in Supplementary Materials and the data are shown in Figure 4a. The initial ε_{Hf} values were calculated back to the average zircon crystallization ages of each sample. The analyzed grains had variable Hf isotopic compositions ranging from positive to strongly negative initial ε_{Hf} values. Fifteen zircon grains from sample XL02 gave initial $^{176}Hf/^{177}Hf$ ratios of 0.280744 to 0.282002. Their initial ε_{Hf} values varied from −19.7 to −8.2 and T_{DM} values from 2.31 to 4.07 Ga. Eighteen zircon grains were analyzed for each sample XL06 and XL23, respectively. These grains yielded initial $^{176}Hf/^{177}Hf$ ratios of 0.282310 to 0.282542. Most of them had positive initial ε_{Hf} values between 0.7 and 8.8 and T_{DM} values of 1.01 Ga to 1.32 Ga. Only one grain gave a negative initial ε_{Hf} value of −0.4 with a T_{DM} value of 1.66 Ga.

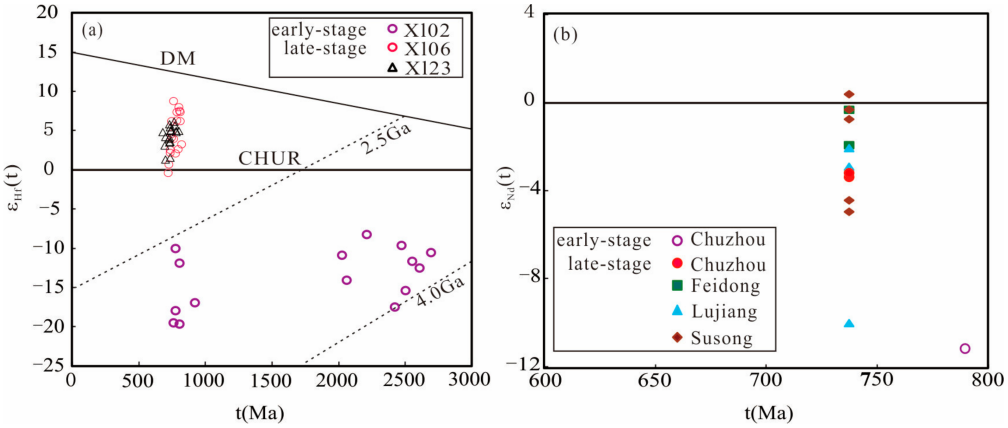

Figure 4. Plots of (**a**) zircon initial ε_{Hf} value versus formation age; (**b**) whole-rock initial ε_{Nd} value versus formation age for volcanic rocks of the Xileng Formation. DM: depleted mantle; CHUR: chondritic uniform reservoir.

Based on the results of the zircon ages and Hf isotopic compositions mentioned above, we subdivide the volcanic rocks of the Xileng Formation into two stages: the early-stage of ~790 Ma and the late-stage of 760–700 Ma peaking at ca. 740 Ma.

4.2. Whole-Rock Geochemical and Nd-Pb Isotopic Compositions

Whole-rock major and trace elemental contents for seventeen samples of meta-volcanic rocks are given in the Table S3 in Supplementary Materials. They include two samples chosen from the early-stage volcanic rocks and fifteen from the late-stage volcanic rocks.

The early-stage volcanic rocks had high SiO2 (66.78 wt.%–68.95 wt.%) and Al2O3 (15.37 wt.%–15.9 wt.%) and low MgO contents (0.69 wt.%–0.9 wt.%). Two samples (XL13 and XL18) had low Na_2O and very high K_2O-contents, and correspondingly high K_2O/Na_2O ratios. Most of the late-stage volcanic rocks showed similar geochemical characteristics in major elements to those of the early-stage volcanic rocks, with high SiO2 (67.4 wt.%–78.5 wt.%) and Al2O3 (12.6 wt.%–19.0 wt.%) and low MgO (0.03 wt.%–0.93 wt.%) contents. In the Nb/Y versus Zr/TiO2 diagram, the early-stage volcanic rocks are dominated by rhyolite and dacite (Figure 5a), while the late-stage volcanic rocks are dominated by trachyandesite. In the FeO versus FeO/MgO diagram, most volcanic rocks belong to the calc-alkaline series (Figure 5b).

In the chondrite-normalized REE patterns (Figure 6a), the early-stage volcanic rocks exhibited low REE contents, highly fractionated REE patterns (LREEs/HREEs of 8.1 to 16.5, $(La/Yb)_N$ of 24.6 to 36.7), and variable Eu/Eu* values of 0.81 to 1.32. The late-stage volcanic rocks had relatively high REE contents, moderately fractionated REE patterns (LREEs/HREEs of 3.5 to 9.1, $(La/Yb)_N$ of 2.4 to 9.7), and more negative Eu-anomalies (Eu/Eu* values of 0.54 to 1.06). In the primitive mantle–normalized trace element diagram (Figure 6b), all the volcanic rocks were significantly enriched in large ion lithophile elements (LILEs) and Pb but depleted in P and Ti; they also showed slightly negative Nb-Ta

anomalies, but positive Zr-Hf anomalies. The early-stage volcanic rocks had significantly higher Sr contents and Sr/Y ratios (Sr/Y of 16 to 66) and fell in the adakitic area when plotted in the $(La/Yb)_N$ versus Yb_N diagram (not shown here). Combined with low MgO contents, they were of low-Mg adakitic affinity.

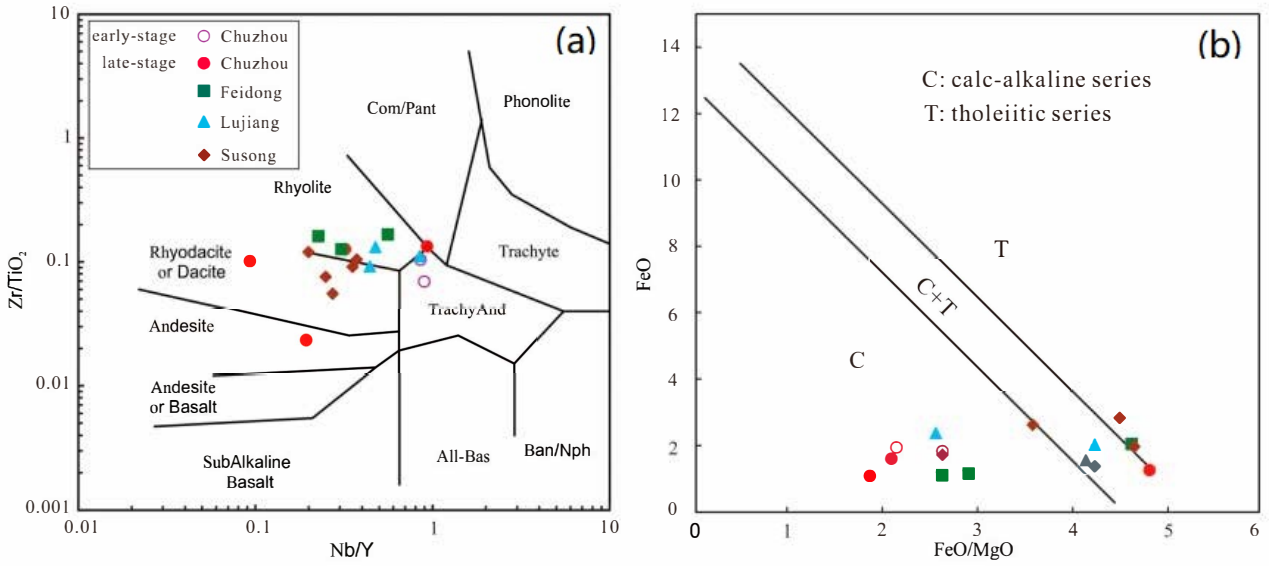

Figure 5. (**a**) Zr/TiO_2 versus Nb/Y diagram after [35] and (**b**) FeO versus FeO/MgO diagram after [36] for volcanic rocks of the Xileng Formation.

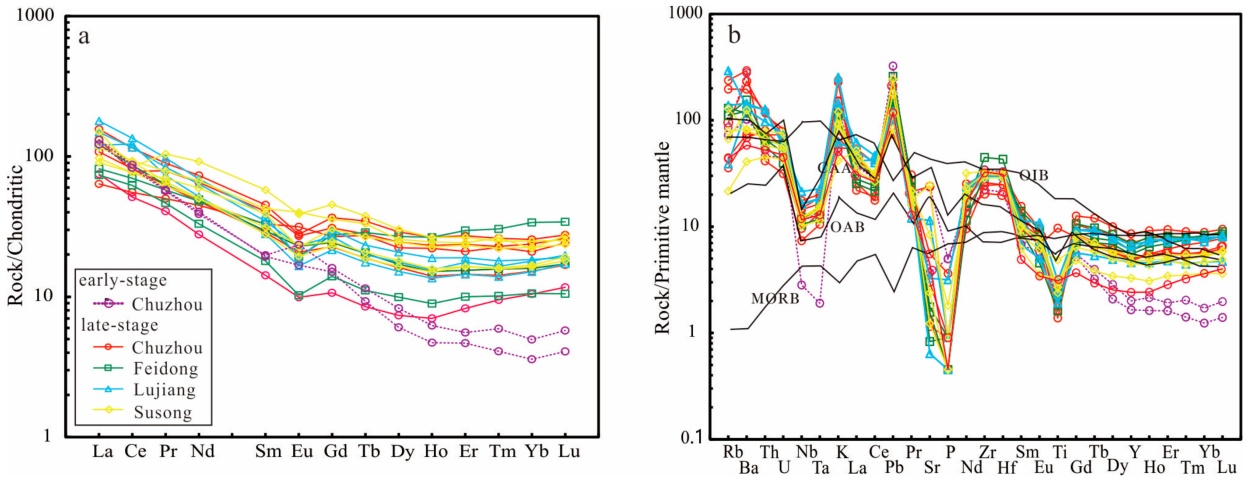

Figure 6. (**a**) Chondrite-normalized rare earth element diagram, and (**b**) primitive mantle-normalized element spider diagram for volcanic rocks of the Xileng Formation. Data of OIB (ocean island basalt), OAB (oceanic arc basalt), CAA (continental arc andesite), and MORB (mid-ocean ridge basalt) after [37]; normalization values from [38].

Whole-rock Nd and Pb isotopic data of thirteen volcanic rock samples are given in the Table S4 in Supplementary Materials. Sample XL02 of the early-stage volcanic rock had a low initial ε_{Nd} value of −11.0 (T_{DM2} age of 2.35 Ga) and low initial Pb isotopic ratios ($^{206}Pb/^{204}Pb$ of 15.91, $^{207}Pb/^{204}Pb$ of 15.32, and $^{208}Pb/^{204}Pb$ of 36.38). Samples of the late-stage volcanic rocks had relatively high initial ε_{Nd} values of −4.6 to +0.5, except for sample XL20 (Figure 4b), when calculated back to 740 Ma. They displayed similar initial Pb isotopic compositions, i.e., $^{206}Pb/^{204}Pb$ of 16.15–17.08, $^{207}Pb/^{204}Pb$ of 15.43–15.51, and $^{208}Pb/^{204}Pb$ of 36.72–37.33 (Figure 7).

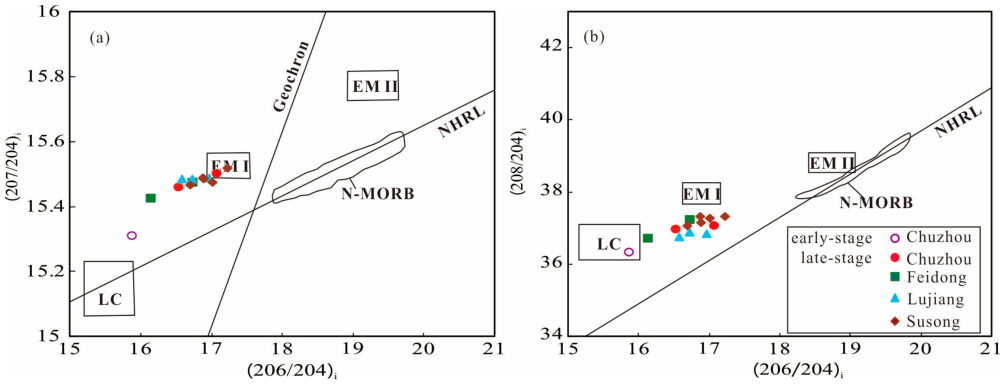

Figure 7. Plots of initial Pb isotopic ratios for volcanic rocks of the Xileng Formation: (**a**) $^{207}Pb/^{204}Pb$ versus $^{206}Pb/^{204}Pb$; (**b**) $^{208}Pb/^{204}Pb$ versus $^{206}Pb/^{204}Pb$. LC: lower crust; EM: enriched mantle; N-MORB: normal mid-ocean ridge basalt; NHRL: northern hemisphere reference line.

5. Discussion

The formation ages of the low-grade metamorphosed volcano-sedimentary rocks in the Zhangbaling uplift are crucial for understanding the tectonic evolution of the northeastern Yangtze Block during the Neoproterozoic. Traditionally, the protolith's age for the Xileng Formation of the Zhangbaling Group was proposed to be early Neoproterozoic (975–925 Ma) [15,16], or middle Neoproterozoic (762–723 Ma) [17–19,39–41]. The sedimentary sequences of the Beijiangjun Formation were assumed to have formed in the Paleo- to Meso-Proterozoic [14]. Recent studies have shown that the Beijiangjun Formation was deposited in the late Neoproterozoic after the Xileng Formation [19].

Most of the volcanic rocks analyzed in this study contained concordant $^{206}Pb/^{238}U$ ages, clustering at two age peaks of ca. 790 and ca. 740 Ma. One volcanic rock (sample XL02) recorded an earlier formation at ca. 790 Ma and contained very old Paleo-Archean to Paleo-Proterozoic (3390 Ma to 2026 Ma) zircon grains. This volcanic rock was geochemically different from other rocks in elemental and Nd-Hf-Pb isotopic compositions. Based on these features, as summarized in Table 1, we can propose two magmatic stages in ~790 Ma and ~760–700 Ma (peaking at ~740 Ma) for the volcanic rocks in the Zhangbaling uplift. In addition, the sedimentary rocks of the Beijiangjun Formation and the overlying strata contained many young 700 Ma to ~630 Ma detrital zircon grains (unpublished data). Therefore, we tentatively conclude that a long-lived, and possibly multiple-stage, magmatism might have taken place along the northeastern margin of the Yangtze block.

Two major stages of magmatism of ~830–800 Ma and ~780–740 Ma are widely distributed along the northern and western margins of the Yangtze Block and were interpreted as related to the evolution of Rodinia [1]. In the present study, Neoproterozoic volcanic rocks of ~790 Ma and ~760–700 Ma (peaking at ~740 Ma) could be discriminated from the Xileng Formation of the Zhangbaling Group. These magmatic activities roughly coincide with the major magmatic episodes in the Yangtze Block. Therefore, the origin of these volcanic rocks can provide valuable information for the tectonic evolution of the northeastern margin of the Yangtze Block during the Neoproterozoic.

The volcanic rocks of the Xileng Formation showed similar geochemical characteristics of arc rocks and most of them belong to the calc-alkaline series. They had highly fractionated REE patterns, negative to weakly positive Eu-anomalies, and were significantly enriched in large ion lithophile elements. However, many differences in geochemical characteristics of trace elements and Nd-Pb-Hf isotopes could be observed between the early-stage (~790 Ma) and late-stage (~760–700 Ma) volcanic rocks.

The trace elemental characteristics of the early-stage volcanic rocks were similar to those of low-Mg adakitic rocks, which are generally interpreted as the products of partial melting of a thickened, garnet-bearing lower crust [42]. They had low initial ε_{Nd} values and low initial Pb isotopic ratios, close to those of ancient basement rocks in the lower

crust. Volcanic rock sample XL02 contained many Archean-Paleoproterozoic (~3.4–2.0 Ga) zircon grains, having very low initial ε_{Hf} values (−19.7 to −8.2). These features point to an origin from melting of ancient basement rocks of the lower crust for the early-stage magmatism. The representative Archean igneous rocks in the eastern Yangtze Block are TTG gneisses in the Kongling area [43–47]. Magmatic zircon grains from the TTG gneisses and other meta-volcanic rocks commonly have negative ε_{Hf} values with Hf model ages of ca. 4.0–3.0 Ga [48–52]. Archean rocks are also exposed in the northern Yangtze Block, documented by ca. 2.8–2.6 Ga TTG rocks in the Yudongzi complex and ~2.5 Ga orthogneisses in the Douling complex [53–55]. Moreover, significant amounts of ~2.5 Ga detrital zircon were reported in Neoproterozoic sedimentary rocks exposed in the Yangtze Block [56]. In combination with the previously reported results, it seems reasonable to conclude that the early-stage volcanic rocks originated from partial melting of ancient rocks underneath the Yangtze Block.

Late-stage volcanic rocks (~760–700 Ma) of the Xileng Formation had arc-like geochemical features in trace elements, which were characterized by enrichment of LILEs and LREEs and depletion of HFSEs in the primitive mantle-normalized spider diagrams [57]. These rocks had relatively high initial ε_{Nd} values and high Pb isotopic ratios compared with those of the early-stage volcanic rocks. Almost all the zircon grains from samples XL06 and XL23 had positive initial ε_{Hf} values, obviously different from those of the early-stage volcanic rock (sample XL02). The late-stage volcanic rocks contained two zircon groups with crystallization ages clustering at ~790 Ma and ~740 Ma (Table 1). These old 790 Ma zircon grains had significantly different Hf isotopic compositions from the zircon grains of the early-stage volcanic rocks. This implies that the magma sources of the late-stage volcanic rocks might have some contribution from juvenile materials, probably of ~790 Ma mafic rocks. According to previously reported data, numerous Neoproterozoic mafic rocks exist in the Yangtze Block (Figure 8).

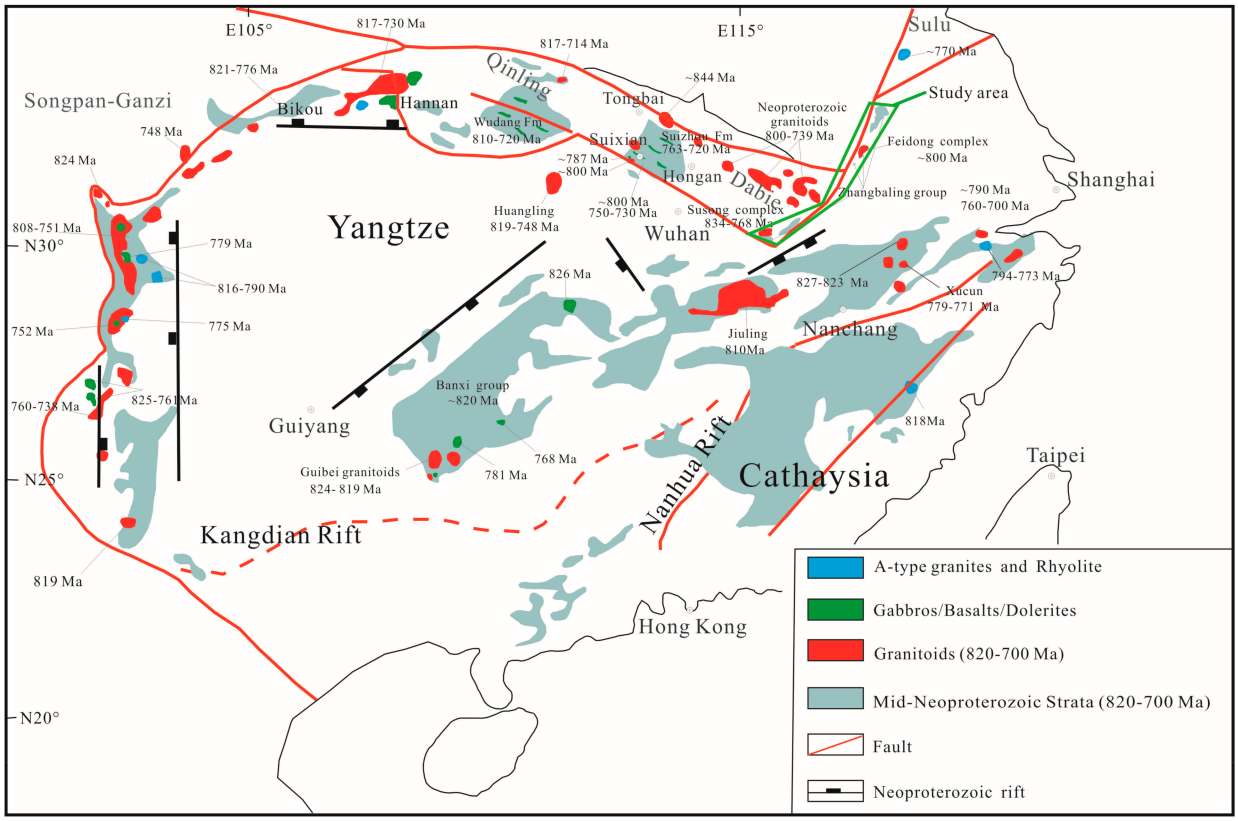

Figure 8. Distribution of Neoproterozoic rocks in south China modified after [58,59].

Three distinctly different models have been proposed to explain the geodynamics of the Neoproterozoic magmatism in the Yangtze Block [60,61]. Neoproterozoic volcanic rocks of the Xileng Formation can be classified in two magmatic stages: ~790 Ma low-Mg adakitic rocks originated from partial melting of ancient basement rocks and ~740 Ma continental arc rocks derived from partial melting of juvenile crustal rocks. Previous studies have identified many subduction–accretion–arc formations in the periphery of the Yangtze Block [62]. Within south China, the coeval (820–720 Ma) rift-related igneous rocks and sedimentary sequences are suggested to have been formed due to long-term subduction along the western margin of the Yangtze Block [63]. Integrating the results of the previous studies, we propose a long-lived magmatism (~820 to ~700 Ma or later) along the northeastern margin of the Yangtze Block. Temporally, it is consistent with the Neoproterozoic magmatism along the northern and western margins of the Yangtze Block [64–66].

6. Conclusions

The low-grade metamorphosed volcano-sedimentary sequences in the Zhangbaling uplift record multiple-stage Neoproterozoic magmatism. Volcanic rocks in the Xileng Formation formed in an early stage of ca. 790 Ma and a late stage of ~760 Ma to ~700 Ma peaking at ca. 740 Ma. Detrital zircon grains in meta-sedimentary rocks of the Xileng Formation and the overlying strata likely record magmatic episodes between ~700 Ma and ~630 Ma. The multiple-stage magmatism recorded in the Zhangbaling uplift might demonstrate a long-lasting subduction along the northeastern margin of the Yangtze Block that lasted until ca. 700 Ma in response to the formation of Rodinia.

The early-stage volcanic rocks contained many Archean to Early Paleoproterozoic zircon grains and had low initial ε_{Nd} and ε_{Hf} values (−11.0; −19.7 to −8.2) and low Pb isotopic ratios. Geochemical features indicated low-Mg adakitic affinities, probably resulting from partial melting of ancient basement rocks underneath the Yangtze Block.

The late-stage volcanic rocks were similar to continental arc rocks in trace element compositions. They had relatively high initial ε_{Nd} and ε_{Hf} values (−9.5 to +0.5; −0.4 to +8.8) and Pb isotopic ratios and most of them contained zircon grains of ~800–790 Ma. The parental magmas of these volcanic rocks might be derived from partial melting mainly of the juvenile mafic crust.

Supplementary Materials: The following supporting information can be downloaded at: https://www.mdpi.com/article/10.3390/min13040562/s1, Table S1: Zircon U-Pb isotopic data obtained by the LA-ICPMS for meta-volcanic rocks from the Xileng Formation; Table S2: Lu-Hf isotopic compositions of zircon grains from volcanic rocks of the Xileng Formation; Table S3: Contents of major (wt.%) and trace (ppm) elements for meta-volcanic rocks from the Xileng Formation; Table S4: Whole rock Nd-Pb isotopic compositions of meta-volcanic rocks from the Xileng Formation; Figure S1: Cathodoluminescence images of representative zircon grains from volcanic rocks of the Xileng Formation.

Author Contributions: J.W. and J.H. designed the study; J.W., Y.Y. and F.C. co-wrote the manuscript; J.W., J.H., J.Z., Y.Y. and F.C. carried out the field work and the analyses. All authors have read and agreed to the published version of the manuscript.

Funding: This study was funded by the National Natural Science Foundation of China (NSFC) (Grant Nos. 42202069 and 41872049).

Data Availability Statement: The authors confirm that the data supporting the findings of this study are available within the article and its Supplementary Materials.

Acknowledgments: Sincere thanks are due to A. Wittmann and two anonymous reviewers for their constructive suggestions, to P. Xiao, J.-F. He and Z.-H. Hou for assistance in analysis, and to H. Zhang and H. Nie for help in fieldwork.

Conflicts of Interest: The authors declare no competing interests.

References

1. Li, Z.X.; Li, X.H.; Kinny, P.D.; Wang, J.; Zhang, S.; Zhou, H. Geochronology of Neoproterozoic syn-rift magmatism in the Yangtze Craton, South China and correlations with other continents: Evidence for a mantle superplume that broke up Rodinia. *Precambrian Res.* **2003**, *122*, 85–109. [CrossRef]
2. Li, X.H.; Li, W.X.; Li, Z.X.; Liu, Y. 850–790 Ma bimodal volcanic and intrusive rocks in northern Zhejiang, South China: A major episode of continental rift magmatism during the breakup of Rodinia. *Lithos* **2008**, *102*, 341–357. [CrossRef]
3. Li, X.H.; Li, W.X.; Li, Q.L.; Wang, X.; Yu, L.; Yang, Y. Petrogenesis and tectonic significance of the ~850 Ma Gangbian alkaline complex in South China: Evidence from in situ zircon U–Pb dating, Hf–O isotopes and whole-rock geochemistry. *Lithos* **2010**, *114*, 1–15. [CrossRef]
4. Wang, J.; Li, Z.X. Sequence stratigraphy and evolution of the Neoproterozoic marginal basins along southeastern Yangtze Craton, South China. *Gondwana Res.* **2001**, *4*, 17–26. [CrossRef]
5. Wang, J.; Li, Z.X. History of Neoproterozoic rift basins in South China: Implications for Rodinia break-up. *Precambrian Res.* **2003**, *122*, 141–158. [CrossRef]
6. Li, Z.X.; Zhang, L.H.; McApowell, C. South China in Rodinia: Part of the missing link between Australia–East Antarctica and Laurentia? *Geology* **1995**, *23*, 407–410. [CrossRef]
7. Piper, J. The Neoproterozoic Supercontinent: Rodinia or Palaeopangaea? *Earth Planet. Sci. Lett.* **2000**, *176*, 131–146. [CrossRef]
8. Meert, J.G.; Torsvik, T.H. The making and unmaking of a supercontinent: Rodinia revisited. *Tectonophysics* **2003**, *375*, 261–288. [CrossRef]
9. Yang, Z.; Sun, Z.; Yang, T.; Pei, J. A long connection (750–380 Ma) between South China and Australia: Paleomagnetic constraints. *Earth Planet. Sci. Lett.* **2004**, *220*, 420–434. [CrossRef]
10. Wang, X.L.; Zhou, J.C.; Qiu, J.S.; Zhang, W.; Liu, X.; Zhang, G. LA–ICP–MS U–Pb zircon geochronology of the Neoproterozoic igneous rocks from northern Guangxi, South China: Implications for tectonic evolution. *Precambrian Res.* **2006**, *145*, 111–130. [CrossRef]
11. Zhou, J.C.; Wang, X.L.; Qiu, J.S. Geochronology of Neoproterozoic mafic rocks and sandstones from northeastern Guizhou, South China: Coeval arc magmatism and sedimentation. *Precambrian Res.* **2009**, *170*, 27–42. [CrossRef]
12. Sun, J.X. On three tectonic questions in Jiangsu Province. *Jiangsu Geol.* **1991**, *15*, 69–76. (In Chinese)
13. Tang, J.F.; Hou, M.J.; Gao, T.S.; Qian, C. Age assignment of the Susong Group, Hongan Group and Haizhou Group: A discussion. *Geol. Bull. China* **2002**, *21*, 166–171. (In Chinese)
14. Hou, M.J.; Wu, Y.d.; Tang, J.F. The metamorphosed stratigraphic succession and structural patterns of the Zhangbaling area. *Geol. Anhui* **1999**, *9*, 26–29. (In Chinese)
15. Guo, K.Y.; Wang, Y.P. Petrology and petrochemistry of the spilite-quartz hornporphyry system in the Zhangbaling metamorphic terrane. *Volcanic Geol. Mineral.* **1995**, *16*, 25–35. (In Chinese)
16. Zhang, D.B.; Guo, K.Y.; Dong, M.X. Geological features of Zhangbaling Group and its division. *Volcanol. Mineral. Resource* **1995**, *16*, 1–16. (In Chinese)
17. Zhao, T.; Zhu, G.; Lin, S.Z.; Yan, L.; Jiang, Q. Protolith ages and deformation mechanism of metamorphic rocks in the Zhangbaling uplift segment of the Tan–Lu fault zone. *Sci. China Ser. D Earth Sci.* **2014**, *11*, 2740–2757. [CrossRef]
18. Shi, Y.H. Petrology and zircon U–Pb geochronology of metamorphic massifs around the middle segment of the Tan-Lu fault to define the boundary between the North and South China blocks. *J. Asian Earth Sci.* **2016**, *141*, 140–160. [CrossRef]
19. Cai, Q.R.; Niu, M.L.; Wu, Q.; Yuan, X.Y.; Wang, T.; Li, X.C.; Sun, Y. Revisiting the formation age of the Zhangbaling Group in the southern segment of the Tan–Lu fault zone. *China J. Geol.* **2019**, *54*, 1–15. (In Chinese)
20. Zheng, J.P.; Dai, H.K.; Zhang, H. Refertilization and replacement of lithospheric mantle beneath the eastern China. *Bull. Mineral. Petrol. Geochem.* **2019**, *2*, 201–216.
21. Zhu, G.; Liu, G.S.; Niu, M.L.; Xie, C.; Wang, Y.; Xiang, B. Syn–collisional transform faulting of the Tan–Lu Fault Zone, East China. *Int. J. Earth Sci.* **2009**, *98*, 135–155. [CrossRef]
22. Niu, M.L.; Yu, H.; Wang, T.; Qi, W.; Li, X.; Zhu, G. Geochronological evidence for the middle early cretaceous strike-slip movement from the Feidong segment of the Tan–Lu fault zone. *Adv. Earth Sci.* **2015**, *30*, 922–939.
23. Zhang, Q.; Jim, D.; Zhu, G. Oblique collision between North and South China recorded in Zhangbaling and Fucha Shan (Dabie–Sulu transfer zone). *Geol. Soc. Am.* **2007**, *434*, 167–206.
24. Zhu, Q.; Wu, L.B.; Du, J.G.; Hu, Z.; Shi, K.; Sun, M.; Zhao, X.; Gao, S. Determination of the Early Cretaceous metamorphic core complex in Zhangbaling Uplift: Constraints on the Tan-Lu fault and its relationship with metallogenesis. *Geol. China* **2019**, *48*, 1639–1652. (In Chinese)
25. Chen, F.; Li, X.H.; Wang, X.L.; Li, Q.; Siebel, W. Zircon age and Nd-Hf isotopic composition of the Yunnan Tethyan belt, southwestern China. *Int. J. Earth Sci.* **2007**, *96*, 1179–1194. [CrossRef]
26. Yuan, H.L.; Gao, S.; Liu, X.M.; Li, H.; Günther, D.; Wu, F. Accurate U–Pb age and trace element determinations of zircon by laser ablation-inductively coupled plasma mass spectrometry. *Geostand. Geoanal. Res.* **2004**, *28*, 353–370. [CrossRef]
27. Griffin, W.L.; Powell, W.J.; Pearson, N.J.; O'Reilly, S.Y. *GLITTER: Data Reduction Software for Laser Ablation ICP-MS*; Mineralogical Association of Canada: Quebec, QC, Canada, 2008.
28. Andersen, T. Correction of common lead in U–Pb analyses that do not report Pb-204. *Chem. Geol.* **2002**, *192*, 59–79. [CrossRef]

29. Ludwig, K.R. *ISOPLOT 3: A Geochronological Toolkit for Microsoft Excel*; Geochronology Centre Special Publication: Berkeley, CA, USA, 2003; 74p.
30. Wu, F.Y.; Yang, Y.H.; Xie, L.W.; Yang, J.; Xu, P. Hf isotopic compositions of the standard zircons and baddeleyites used in U–Pb geochronology. *Chem. Geol.* **2006**, *234*, 105–126. [CrossRef]
31. Iizuka, T.; Hirata, T.; Komiya, T.; Rino, S.; Katayama, I.; Motoki, A.; Maruyama, S. U–Pb and Lu–Hf isotope systematics of zircons from the Mississippi River sand: Implications for reworking and growth of continental crust. *Geology* **2005**, *33*, 485–488. [CrossRef]
32. Rubatto, D. Zircon trace element geochemistry: Partitioning with garnet and the link between U–Pb ages and metamorphism. *Chem. Geol.* **2002**, *184*, 123–138. [CrossRef]
33. Bingen, B.; Austrheim, H.; Whitehouse, M.J.; Davis, W.J. Trace element signature and U–Pb geochronology of eclogite–facies zircon, Bergen Arcs, Caledonides of W Norway. *Contrib. Mineral. Petrol.* **2004**, *147*, 671–683. [CrossRef]
34. Dickinson, W.R.; Gehrels, G.E. U–Pb ages of detrital zircons from Permian and Jurassic eolian sandstones of the Colorado Plateau, USA: Paleogeographic implications. *Sediment. Geol.* **2003**, *163*, 29–66. [CrossRef]
35. Winchester, J.A.; Floyd, P.A. Geochemical discrimination of different magma series and their differentiation products using immobile elements. *Chem. Geol.* **1977**, *20*, 325–343. [CrossRef]
36. Miyashiro, A. Volcanic rock series in island arcs and active continental margins. *Am. J. Sci.* **1974**, *274*, 321–355. [CrossRef]
37. Kelemen, P.B.; Hanghj, K.; Greene, A.R. One view of the geochemistry of subduction-related magmatic arcs, with an emphasis on primitive andesite and lower crust. *Treatise Geochem.* **2007**, *3*, 659.
38. Sun, S.S.; McDonough, W.F. Chemical and isotopic systematics of oceanic basalts: Implications for mantle composition and processes. *Geol. Soc. Lond. Spec. Publ.* **1989**, *42*, 313–345. [CrossRef]
39. Yang, G.S.; Shi, J.F.; Shi, Y.H.; Wang, J.; Li, Y. Evaluation of the main stage metamorphism temperature of the Zhangbaling group in eastern Anhui and its structural framework. *Chin. J. Geol.* **2019**, *3*, 736–762. (In Chinese)
40. Zhu, Q.; Shi, K.; Wu, L.B.; Jiang, L.; Hu, Z.; Xu, S.; Weng, W. Continued subduction of the Yangtze Plate in the Middle Neoproterozoic: New evidence based on the geochronology and petro–geochemistry of island arc volcanic rocks in the Nanhua Period. *Earth Sci. Front.* **2020**, *4*, 17–32. (In Chinese)
41. Cai, Q.R.; Niu, M.L.; Yuan, X.Y.; Wu, Q.; Zhu, G.; Li, X.C.; Sun, Y.; Li, C. Evidence for continental rifting from two episodes of Mid–Neoproterozoic silicic magmatism in the northeastern Yangtze block, China. *Precambrian Res.* **2021**, *363*, 106336. [CrossRef]
42. Atherton, M.P.; Petford, N. Generation of sodium-rich magmas from newly underplated basaltic crust. *Nature* **1993**, *362*, 144–146. [CrossRef]
43. Jiao, W.F.; Wu, Y.B.; Yang, S.H.; Peng, M.; Wang, J. The oldest basement rock in the Yangtze Craton revealed by zircon U–Pb age and Hf isotope composition. *Sci. China Series D Earth Sci.* **2009**, *52*, 1393–1399. [CrossRef]
44. Guo, J.L.; Gao, S.; Wu, Y.B.; Li, M.; Chen, K.; Hu, Z.; Liang, Z.; Liu, Y.; Zhou, L.; Zong, K.; et al. 3.45 Ga granitic gneisses from the Yangtze Craton, South China: Implications for Early Archean crustal growth. *Precambrian Res.* **2014**, *242*, 82–95. [CrossRef]
45. Guo, J.L.; Wu, Y.B.; Gao, S.; Jin, Z.; Zong, K.; Hu, Z.; Chen, K.; Chen, H.; Liu, Y. Episodic Paleoarchean-Paleoproterozoic (3.3–2.0 Ga) granitoid magmatism in Yangtze Craton, South China: Implications for late Archean tectonics. *Precambrian Res.* **2015**, *270*, 246–266. [CrossRef]
46. Wang, K.; Li, Z.X.; Dong, S.; Cui, J.; Han, B.; Zheng, T.; Xu, Y. Early crustal evolution of the Yangtze Craton, South China: New constraints from zircon U–Pb–Hf isotopes and geochemistry of ca. 2.9–2.6 Ga granitic rocks in the Zhongxiang Complex. *Precambrian Res.* **2018**, *314*, 325–352. [CrossRef]
47. Qiu, X.F.; Ling, W.L.; Liu, X.M.; Lu, S.; Jiang, T.; Wei, Y.; Peng, L.; Tan, J. Evolution of the Archean continental crust in the nucleus of the Yangtze block: Evidence from geochemistry of 3.0 Ga TTG gneisses in the Kongling high–grade metamorphic terrane, South China. *J. Asian Earth Sci.* **2018**, *154*, 149–161. [CrossRef]
48. Zhang, S.B.; Zheng, Y.F.; Wu, Y.B.; Zhao, Z.; Gao, S.; Wu, F. Zircon U–Pb age and Hf isotope evidence for 3.8 Ga crustal remnant and episodic reworking of Archean crust in South China. *Earth Planet. Sci. Lett.* **2006**, *252*, 56–71. [CrossRef]
49. Zheng, J.P.; Griffin, W.L.; O'Reilly, S.Y.; Zhang, M.; Pearson, N.J.; Pan, Y. Widespread Archean basement beneath the Yangtze craton. *Geology* **2006**, *34*, 417–420. [CrossRef]
50. Gao, S.; Yang, J.; Zhou, L.; Li, M.; Hu, Z.; Guo, J.; Yuan, H.; Gong, H.; Xiao, G.; Wei, J. Age and growth of the Archean Kongling terrain, South China, with emphasis on 3.3 Ga granitoid gneisses. *Am. J. Sci.* **2011**, *311*, 153–182. [CrossRef]
51. Chen, K.; Gao, S.; Wu, Y.B.; Guo, J.; Hu, Z.; Liu, Y.; Zong, K.; Liang, Z.; Geng, X. 2.6–2.7 Ga crustal growth in Yangtze craton, South China. *Precambrian Res.* **2013**, *224*, 472–490. [CrossRef]
52. Li, Y.H.; Zheng, J.P.; Xiong, Q.; Wang, W.; Ping, X.; Li, X.; Tang, H. Petrogenesis and tectonic implications of Paleoproterozoic metapelitic rocks in the Archean Kongling Complex from the northern Yangtze Craton, South China. *Precambrian Res.* **2016**, *276*, 158–177. [CrossRef]
53. Nie, H.; Yao, J.; Wan, X.; Zhu, X.; Siebel, W.; Chen, F. Precambrian tectonothermal evolution of South Qinling and its affinity to the Yangtze Block: Evidence from zircon ages and Hf–Nd isotopic compositions of basement rocks. *Precambrian Res.* **2016**, *286*, 167–179. [CrossRef]
54. Zhou, G.Y.; Wu, Y.B.; Li, L.; Zhang, W.; Zheng, J.; Wang, H.; Yang, S. Identification of ca. 2.65 Ga TTGs in the Yudongzi complex and its implications for the early evolution of the Yangtze Block. *Precambrian Res.* **2018**, *314*, 240–263. [CrossRef]

55. Chen, Q.; Sun, M.; Zhao, G.C.; Zhao, J.; Zhu, W.; Long, X.; Wang, J. Episodic crustal growth and reworking of the Yudongzi terrane, South China: Constraints from the Archean TTGs and potassic granites and Paleoproterozoic amphibolites. *Lithos* **2019**, *326–327*, 1–18. [CrossRef]
56. Wang, X.; Guo, J.W.; Tao, W.; Jiang, L.; Deng, J.; Ma, C. Paleoproterozoic tectonic evolution of the Yangtze Craton: Evidence from magmatism and sedimentation in the Susong area, South China. *Precambrian Res.* **2021**, *365*, 106390. [CrossRef]
57. Zhao, J.H.; Zhou, M.F. Neoproterozoic adakitic plutons and arc magmatism along the western margin of the Yangtze Block, South China. *J. Geol.* **2007**, *115*, 675–689. [CrossRef]
58. Wang, L.J.; Yu, J.H.; Griffin, W.L.; O'Reilly, S.Y. Early crustal evolution in the western Yangtze Block: Evidence from U–Pb and Lu–Hf isotopes on detrital zircons from sedimentary rocks. *Precambrian Res.* **2012**, *222–223*, 368–385. [CrossRef]
59. Yang, Y.N.; Wang, X.C.; Li, Q.L.; Li, X. Integrated in situ U–Pb age and Hf–O analyses of zircon from Suixian Group in northern Yangtze: New insights into the Neoproterozoic low–$\delta^{18}O$ magmas in the South China Block. *Precambrian Res.* **2016**, *273*, 151–164. [CrossRef]
60. Zhou, M.F.; Yan, D.P.; Kennedy, A.K.; Li, Y.Q.; Ding, J. SHRIMP U–Pb zircon geochronological and geochemical evidence for Neoproterozoic arc–magmatism along the western margin of the Yangtze Block, South China. *Earth Planet. Sci. Lett.* **2002**, *196*, 51–67. [CrossRef]
61. Dong, Y.; Santosh, M. Tectonic architecture and multiple orogeny of the Qinling Orogenic Belt, Central China. *Gondwana Res.* **2016**, *29*, 1–40. [CrossRef]
62. Xu, Y.; Yang, K.G.; Polat, A.; Yang, Z. The 860 Ma mafic dikes and granitoids from the northern margin of the Yangtze Block, China: A record of oceanic subduction in the early Neoproterozoic. *Precambrian Res.* **2016**, *275*, 310–331. [CrossRef]
63. Zhao, J.H.; Zhou, M.F.; Yan, D.P.; Zheng, J.; Li, J. Reappraisal of the ages of Neoproterozoic strata in South China: No connection with the Grenvillian orogeny. *Geology* **2011**, *39*, 299–302. [CrossRef]
64. Dong, Y.P.; Liu, X.M.; Santosh, M.; Chen, Q.; Zhang, X.; Li, W.; He, D.; Zhang, G. Neoproterozoic accretionary tectonics along the northwestern margin of the Yangtze Block, China: Constraints from zircon U–Pb geochronology and geochemistry. *Precambrian Res.* **2012**, *196–197*, 247–274. [CrossRef]
65. Zhu, Y.; Lai, S.C.; Qin, J.F.; Zhu, R.; Yang, H. Neoproterozoic metasomatized mantle beneath the western Yangtze Block, South China: Evidence from whole–rock geochemistry and zircon U–Pb–Hf isotopes of mafic rocks. *J. Asian Earth Sci.* **2020**, *206*, 104616. [CrossRef]
66. Gao, F.; Pei, X.; Li, R.; Li, Z.; Pei, L.; Chen, Y.; Chen, Y.; Wang, M.; Zhao, S.; Liu, C.; et al. Neoproterozoic tectonic evolution of the northwestern margin of the Yangtze block (southwestern China): Evidence from sandstone geochemistry and detrital zircon U–Pb ages of the Hengdan Group. *Precambrian Res.* **2020**, *344*, 105737. [CrossRef]